1 Introduction

1.1 Coordinate System

We use a downward-facing right-handed Cartesian coordinate system. For spherical coordinates, we denote polar declenation from the positive z axis by ϕ and azimuthal angle from the positive x-axis towards the positive y-axis by θ.

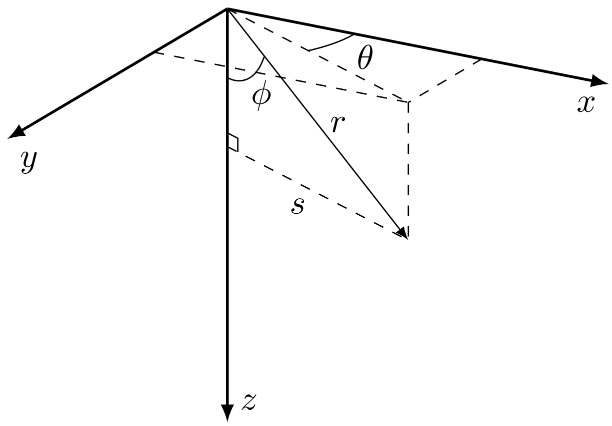

Figure 1: Spatial grid

1.2 Domain

Let the domain be defined as

$$\begin{aligned} D = \big\{\mathbf{x} \in \mathbb{R}^3 : x_{\text{min}} &\leq \mathbf{x} \cdot \hat{x} \leq x_{\text{max}} \\ \text{and } y_{\text{min}} &\leq \mathbf{x} \cdot \hat{y} \leq y_{\text{max}} \\ \text{and } z_{\text{min}} &\leq \mathbf{x} \cdot \hat{z} \leq z_{\text{max}}\big\} \end{aligned} \tag{1}$$

Let the surface and bottom of the domain be denoted respectively by

$$S = \{\mathbf{x_s} \in D : \mathbf{x_s} \cdot \hat{z} = 0\} \tag{2}$$
$$B = \{\mathbf{x_b} \in D : \mathbf{x_b} \cdot \hat{z} = 0\} \tag{3}$$

1.3 Assumptions

We assume that the scattering coefficient is constant over space; that the primary difference in the optical effects of kelp and water is absorption, not scattering.

- Scattering constant (same for kelp/water)

1.4 Table of variables

2 Asymptotics Motivation

2.1 Limitations of Discrete Ordinates

- All angles are coupled by integral
- GMRES is very memory-intensive.
- It's very CPU-intensive as well.
- It also might never converge!
- Especially if we start from zero.

2.2 Advantages of Asymptotics

- Solve each angular problem independently
- Relatively computationally cheap
- Much lower memory cost
- Known number of operations
- Low and high accuracy available

3 RTE Formulation

3.1 RTE: 1D

Consider a fixed position $\mathbf{x}$ and direction ω such that $\omega \cdot \hat{z} \neq 0$.

** Just call $\mathbf{x_0}$ a point, not a function. Call it the projection to the surface.

Let $\mathbf{l}(\mathbf{x}, \omega, s)$ denote the linear path containing $\mathbf{x}$ with initial z coordinate given by

$$z_0 = \begin{cases} 0, & \omega \cdot \hat{z} < 0 \\ z_{\text{max}}, & \omega \cdot \hat{z} > 0 \end{cases} \tag{4}$$

Then,

$$\mathbf{l}(\mathbf{x}, \omega, s) = \frac{1}{\tilde{s}}(s\mathbf{x} + (\tilde{s} - s)\mathbf{x_0}(\mathbf{x}, \omega)) \tag{5}$$

where

$$\mathbf{x_0}(\mathbf{x}, \omega) = \mathbf{x} - \tilde{s}\omega \tag{6}$$

is the origin of the ray, and

$$\tilde{s} = \frac{\mathbf{x} \cdot \hat{z} - z_0}{\omega \cdot \hat{z}} \tag{7}$$

is the path length from $\mathbf{x_0}(\mathbf{x}, \omega)$ to $\mathbf{x}$.

3.2 Colloquial Description

Denote the radiance at $\mathbf{x}$ in the direction ω by $L(\mathbf{x}, \omega)$. As light travels along $\mathbf{l}(\mathbf{x}, \omega, s)$, interaction with the medium produces three phenomena of interest:

1. Radiance is decreased due to absorption.
2. Radiance is decreased due to scattering out of the path to other directions.
3. Radiance is increased due to scattering into the path from other directions.

3.3 IOPs

These phenomena are governed by three inherent optical properties (IOPs) of the medium. The absorption coefficient $a(\mathbf{x})$ (units m^{-1}) defines the proportional loss of radiance per unit length. The scattering coefficient b (units m^{-1}), defines the proportional loss of radiance per unit length, and is assumed to be constant over space.

The volume scattering function (VSF) $\beta(\Delta) : [0, \pi] \to \mathbb{R}^+$ (units sr^{-1}) defines the proportion of radiance scattered at an angle Δ from it's original direction. The VSF is normalized such that $\int_0^\pi \beta(\Delta)\, d\Delta = 1$. The scattering coefficient b can be considered the magnitude of the unnormalized VSF.

3.4 Equation of Transfer

Then, combining these phenomena, the Radiative Transfer equation along $\mathbf{l}(\mathbf{x}, \omega)$ becomes

$$\frac{dL}{ds}(\mathbf{l}(\mathbf{x}, \omega, s), \omega) = -(a(\mathbf{x}) + b)L(\mathbf{x}, \omega) + b \int_{4\pi} \beta(|\omega - \omega'|)L(\mathbf{x})\, d\omega', \tag{8}$$

where $\int_{4\pi}$ denotes integration over the unit sphere and $|\omega - \omega'| = \cos^{-1}(|\omega - \omega'|)$.

3.5 RTE: Vector

Now, we have

$$\begin{aligned}\frac{dL}{ds}(\mathbf{l}(\mathbf{x}, \omega, s), \omega) &= \frac{d\mathbf{l}}{ds}(\mathbf{x}, \omega, s) \cdot \nabla L(\mathbf{x}, \omega', \omega) \\ &= \omega \cdot \nabla L(\mathbf{x}, \omega)\end{aligned}$$

Then, the general form of the Radiative Transfer Equation is

$$\omega \cdot \nabla L(\mathbf{x}, \omega) = -(a(\mathbf{x}) + b)L(\mathbf{x}, \omega) + b \int_{4\pi} \beta(|\omega - \omega'|)L(\mathbf{x}, \omega')\, d\omega' \tag{9}$$

or, equivalently,

$$\omega \cdot \nabla L(\mathbf{x}, \omega) + a(\mathbf{x})L(\mathbf{x}, \omega) = b\left(\int_{4\pi} \beta(|\omega - \omega'|)L(\mathbf{x}, \omega')\, d\omega' - L(\mathbf{x}, \omega)\right) \tag{10}$$

4 Asymptotics

4.1 Substitute asymptotic series

$$L(\mathbf{x}, \omega) = L_0(\mathbf{x}, \omega) + bL_1(\mathbf{x}, \omega) + b^2 L_2(\mathbf{x}, \omega) + \cdots \tag{11}$$

Then, substituting the above into the RTE,

$$\begin{aligned}\omega \cdot \nabla \left[L_0(\mathbf{x}, \omega) + bL_1(\mathbf{x}, \omega) + b^2 L_2(\mathbf{x}, \omega) + \cdots\right] + a(\mathbf{x}) \left[L_0(\mathbf{x}, \omega) + bL_1(\mathbf{x}, \omega) + b^2 L_2(\mathbf{x}, \omega) + \cdots\right] \\ = b\Bigg(\int_{4\pi} \beta(|\omega - \omega'|) \left[L_0(\mathbf{x}, \omega') + bL_1(\mathbf{x}, \omega') + b^2 L_2(\mathbf{x}, \omega') + \cdots\right] d\omega' \\ - \left[L_0(\mathbf{x}, \omega) + bL_1(\mathbf{x}, \omega) + b^2 L_2(\mathbf{x}, \omega) + \cdots\right] \Bigg)\end{aligned} \tag{12}$$

Now, grouping like powers of b, we have the decopled set of equations

$$\omega \cdot \nabla L_0(\mathbf{x}, \omega) + a(\mathbf{x})L_0(\mathbf{x}) = 0 \tag{13}$$

$$\omega \cdot \nabla L_1(\mathbf{x}, \omega) + a(\mathbf{x})L_1(\mathbf{x}) = \int_{4\pi} \beta(|\omega - \omega'|)L_0(\mathbf{x}, \omega')\, d\omega' - L_0(\mathbf{x}, \omega) \tag{14}$$

$$\omega \cdot \nabla L_2(\mathbf{x}, \omega) + a(\mathbf{x})L_2(\mathbf{x}) = \int_{4\pi} \beta(|\omega - \omega'|)L_1(\mathbf{x}, \omega')\, d\omega' - L_1(\mathbf{x}, \omega) \tag{15}$$

$$\vdots$$

4.2 Boundary Conditions

We use periodic boundary conditions in the x and y directions.

$$L\left((x_{\text{min}}, y, z), \omega\right) = L\left((x_{\text{max}}, y, z), \omega\right) \tag{16}$$

$$L\left((x, y_{\text{min}}, z), \omega\right) = L\left((x, y_{\text{max}}, z), \omega\right) \tag{17}$$

In the z direction, we specify a spatially uniform downwelling light just under the surface of the water by a function $f(\omega)$.

* z_{min} could also be much lower, e.g. 5m.

Further, we assume that no upwelling light enters the domain from the bottom.

$$L(\mathbf{x_s}, \omega) = f(\omega) \text{ if } \omega \cdot \hat{z} > 0 \tag{18}$$

$$L(\mathbf{x_b}, \omega) = 0 \text{ if } \omega \cdot \hat{z} < 0 \tag{19}$$

4.3 Rewrite as ODE along ray path

For all $\mathbf{x}, \omega$, let

$$\tilde{a}(s) = a(\mathbf{l}(\mathbf{x}, \omega), s), \tag{20}$$

$$\frac{du_0}{ds}(s) + \tilde{a}(s) u_0(s) = 0, u_0(0) = f(\omega) \tag{21}$$

Then,

$$u_0(s) = f(\omega) \exp\left(-\int_0^s \tilde{a}(s)\, ds\right), \tag{22}$$

$$L_0(\mathbf{l}(\mathbf{x}, \omega, s), \omega) = u_0(s) \tag{23}$$

$$g_n(s) = \int_{4\pi} \beta(|\omega - \omega'|) L_{n-1}(\mathbf{l}(\mathbf{x}, \omega', s), \omega')\, d\omega' - L_{n-1}(\mathbf{l}(\mathbf{x}, \omega, s), \omega) \tag{24}$$

$$\frac{du_n}{ds}(s) + \tilde{a}(s) u_n(s) = g_n(s), u_n(0) = 0 \tag{25}$$

Then,

$$u_n(s) = \int_0^s g_n(s') \exp\left(-\int_{s''}^{s'} \tilde{a}(s'')\, ds''\right) ds' \tag{26}$$

$$L_n(\mathbf{l}(\mathbf{x}, \omega, s), \omega) = u_n(s) \tag{27}$$

4.4 Solve ODE as 1st order linear via I.F.

5 Physical Interpretation

6 Numerical Implementation

Following is a description of the uniform, rectangular spatial-angular grid used in the numerical implementation of this model. It is assumed that all simulated quantities are constant over the interior of a grid cell. The following indices are assigned to each dimension:

$$x \to i \tag{28}$$

$$y \to j \tag{29}$$

$$z \to k \tag{30}$$

$$\theta \to l \tag{31}$$

$$\phi \to m \tag{32}$$

Then, the center of a generic grid cell will be denoted as $(x_i, y_j, z_k, \theta_l, \phi_m)$, and the boundaries between adjacent grid cells will be referred to as *edges*. The number of grid points in each dimension are denoted by n_x, n_y, n_z, n_θ, and n_ϕ, with uniform spacings dx, dy, dz, $d\theta$, and $d\phi$ between adjacent grid points. Each dimension has the same number of edges as cells. One-indexing will be employed throughout this document.

6.1 Spatial Grid

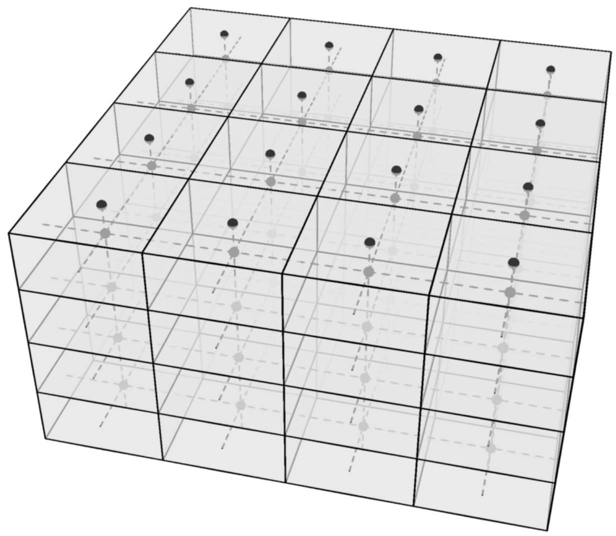

Figure 2: Spatial grid

$$dx = \frac{x_{\max} - x_{\min}}{n_x} \tag{33}$$

$$dy = \frac{y_{\max} - y_{\min}}{n_y} \tag{34}$$

$$dz = \frac{z_{\max} - z_{\min}}{n_z} \tag{35}$$

Then,

$$x_i = (i - 1/2)dx \tag{36}$$

$$y_j = (j - 1/2)dy \tag{37}$$

$$z_k = (k - 1/2)dz \tag{38}$$

6.2 Surface Radiance

Note that 0 is not stored as a grid center in any spatial dimension. Radiance values for the surface boundary condition are stored separately as the four-dimensional array (f_{ijlm}).

6.3 Angular Grid

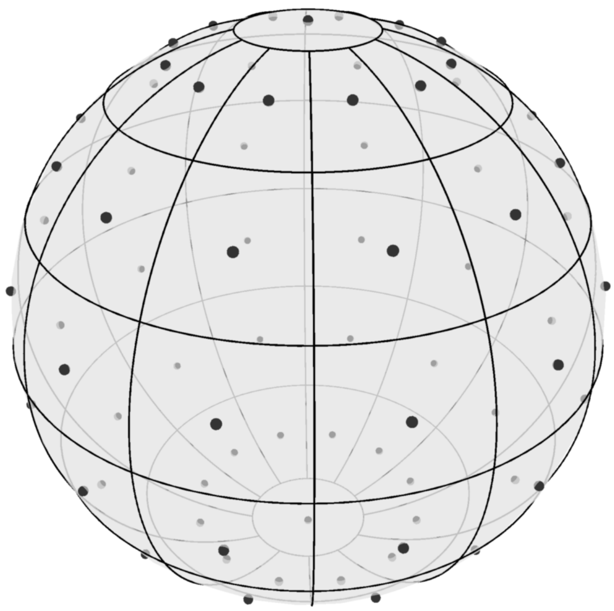

Figure 3: Angular grid

As shown in Figure 3, $\phi = 0$ and $\phi = \pi$ are treated separately. These grid cells are referred to as poles. Accordingly, we have

$$\phi_1 = 0, \tag{39}$$
$$\phi_{n_\phi} = \pi. \tag{40}$$

Meanwhile, θ is similar to the spatial dimensions in that its extreme values are not grid centers.

Then,

$$d\theta = \frac{2\pi}{n_\theta}, \tag{41}$$
$$d\phi = \frac{\pi}{n_\phi - 1}. \tag{42}$$

Then,

$$\theta_l = (l-1)d\theta, \tag{43}$$
$$\phi_m = (m-1)d\phi \tag{44}$$

6.3.1 Storing pole values

We store pole values in the $(1,1)$ and $(1, n_\phi)$ positions.

6.4 Angular Quadrature

We assume that all quantities are constant within a spatial-angular grid cell. We therefore employ the midpoint rule for both spatial and angular integration.

** Need to define $\mathcal{X}$ in this context, I think.

** Is $d\theta$, etc. for both differential and grid spacing confusing?

$$
\begin{aligned}
\int_{4\pi} f(\omega)\, d\omega &= \int_0^{2\pi} \int_0^{\pi} f(\theta,\phi) \sin(\phi)\, d\phi\, d\theta && (45)\\
&\text{**Need to deal with poles separately**} && (46)\\
&= \int_0^{2\pi} \int_0^{\pi} \sum_{l=1}^{n\theta} \sum_{m=1}^{n\phi} f_{lm} \mathcal{X}_l(\theta) \mathcal{X}_m(\phi) \sin(\phi)\, d\phi\, d\theta && (47)\\
&= \sum_{l=1}^{n\theta} \sum_{m=1}^{n\phi} f_{lm} \int_{\theta_l}^{\theta_{l+1}} \int_{\phi_m}^{\phi_{m+1}} \sin(\phi)\, d\phi\, d\theta && (48)\\
&= d\theta \sum_{l=1}^{n\theta} \sum_{m=1}^{n\phi} f_{lm} \int_{\phi_m}^{\phi_{m+1}} \sin(\phi)\, d\phi && (49)\\
&= d\theta \sum_{l=1}^{n\theta} \sum_{m=1}^{n\phi} f_{lm} \left(\cos(\phi_m - d\phi/2) - \cos(\phi_m + d\phi/2)\right) && (50)\\
& && (51)
\end{aligned}
$$

6.5 Ray Tracing Algorithm

6.5.1 Extract values along path

- Path spacing (s)

In order to evaluate a path integral through the previously described grid, it is first necessary to construct a one-dimensional piecewise constant integrand which is discontinuous at unevenly spaced points corresponding to the intersections between the path and edges in the spatial grid.

Consider a grid center $\mathbf{x_1} = (x_1, y_1, z_1)$ and a corresponding path $\mathbf{l}(\mathbf{x_1}, \omega, s)$. To find the location of discontinuities in the itegrand, we first calculate the distance from its origin, $\mathbf{x_0}(\mathbf{x_1}, \omega) = (x_0, y_0, z_0)$ to grid edges in each dimension separately.

** THIS NOTATION IS OVERLOADED **

Given

$$
\begin{aligned}
x_i &= x_0 + s_i^x / \tilde{s}(x_1 - x_0) && (52)\\
y_j &= y_0 + s_j^y / \tilde{s}(y_1 - y_0) && (53)\\
z_k &= z_0 + s_k^z / \tilde{s}(z_1 - z_0) && (54)\\
& && (55)
\end{aligned}
$$

we have

$$
\begin{aligned}
s_i^x &= \tilde{s} \frac{x_i - x_0}{x_1 - x_0} && (56)\\
s_i^y &= \tilde{s} \frac{y_i - y_0}{y_1 - y_0} && (57)\\
s_i^z &= \tilde{s} \frac{z_i - z_0}{z_1 - z_0} && (58)\\
& && (59)
\end{aligned}
$$

Then, move to the adjacent grid cell in the dimension which requires the shortes step to reach an edge. Save ds of the path through this cell. Also save abs. coef. and source. ** Definitely needs more work**

- absorption coefficient ($\tilde{a}(s)$)

- effective source ($g_n(s)$) 0

6.5.2 Ray integral

Let

$$g_n(s) = \sum_{i=1}^{N-1} g_{ni}\mathcal{X}_i(s) \tag{60}$$

$$\tilde{a}(s) = \sum_{i=1}^{N-1} \tilde{a}_i\mathcal{X}_i(s) \tag{61}$$

$$\tag{62}$$

and

$$\mathcal{X}_i(s) = \begin{cases} 1, & a_I \leq s < s_{i+1} \\ 0, & \text{otherwise} \end{cases} \tag{63}$$

and $\{s_i\}_{i=1}^{N}$ is increasing.

Let $ds_i = s_{i+1} - s_i$.

Let $\hat{i}(s) = \min\{i \in \{1, \ldots, N\} : s_i > s\}$. Let $\tilde{d}(s) = s_{\hat{i}(s)} - s$.

We have $s_1 = 0$ and $s_N = \tilde{s}$.

$$u_n(\tilde{s}) = \int_0^{\tilde{s}} g_n(s') \exp\left(-\int_{s''}^{s'} \tilde{a}(s'')\, ds''\right) ds' \tag{64}$$

$$= \int_0^{s_N} \sum_{i=1}^{N-1} g_{ni}\mathcal{X}_i(s') \exp\left(-\int_{s''}^{s'} \sum_{j=1}^{N-1} \tilde{a}_j \mathcal{X}_j(s'')\, ds''\right) ds' \tag{65}$$

$$= \sum_{i=1}^{N-1} g_{ni} \int_0^{s_N} \mathcal{X}_i(s') \exp\left(-\sum_{j=1}^{N-1} \tilde{a}_j \int_{s''}^{s'} \mathcal{X}_j(s'')\, ds''\right) ds' \tag{66}$$

$$= \sum_{i=1}^{N-1} g_{ni} \int_{s_i}^{s_{i+1}} \exp\left(-\tilde{a}_{\hat{i}(s')-1}\tilde{d}(s') - \sum_{j=\hat{i}(s')}^{N-1} \tilde{a}_j ds_j\right) ds' \tag{67}$$

$$= \sum_{i=1}^{N-1} g_{ni} \int_{s_i}^{s_{i+1}} \exp\left(-\tilde{a}_i(s_{i+1} - s') - \sum_{j=i+1}^{N-1} \tilde{a}_j ds_j\right) ds' \tag{68}$$

Let

$$b_i = -\tilde{a}_i s_{i+1} - \sum_{j=i+1}^{N-1} \tilde{a}_j ds_j. \tag{69}$$

Then,

$$u_n(\tilde{s}) = \sum_{i=1}^{N-1} g_{ni} \int_{s_i}^{s_{i+1}} \exp\left(\tilde{a}_i s' + b_i\right)\, ds' \tag{70}$$

Let

$$d_i = \int_{s_i}^{s_{i+1}} \exp\left(\tilde{a}_i s' + b_i\right)\, ds' \tag{71}$$

$$= \begin{cases} ds_i \exp(b_i), & \tilde{a} = 0 \\ \left(\exp(\tilde{a}_i s_{i+1}) - \exp(\tilde{a}_i s_i)\right)/\tilde{a}_i, & \text{otherwise} \end{cases} \tag{72}$$

Then,

$$u_n(\tilde{s}) = \sum_{i=1}^{N-1} g_{ni} d_i \tag{73}$$